AD-A155 222 DETERMINATIÓN OF KINETIC PARAMETERS OF MOLECULAR BEAM EPITAXY(U) FOREIGN TECHNOLOGY DIV WRIGHT-PATTERSON AFB OH J ZHONG 17 APR 85 FTD-ID(RS)T-1601-84 1/1

UNCLASSIFIED F/G 20/12 NL

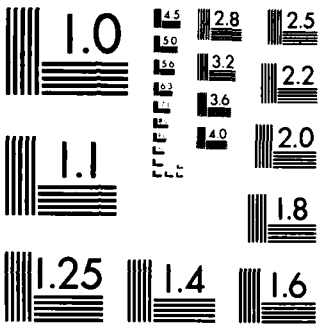

FTD-ID(RS)T-1601-84

FOREIGN TECHNOLOGY DIVISION

DETERMINATION OF KINETIC PARAMETERS OF MOLECULAR BEAM EPITAXY

BY

Zhong Jingchang

EDITED TRANSLATION

FTD-ID(RS)T-1601-84 17 April 1985

MICROFICHE NR: FTD-85-C-000239

DETERMINATION OF KINETIC PARAMETERS OF MOLECULAR BEAM EPITAXY

By: Zhong Jingchang

English pages: 13

Source: Guangxue Xuebao Vol. 4, Nr. 3, March 1984, pp. 257-263

Country of origin: China
Translated by: SCITRAN
F33657-84-D-0165
Requester: FTD/TQTR

PREPARED BY:

TRANSLATION DIVISION
FOREIGN TECHNOLOGY DIVISION
WP-AFB, OHIO.

GRAPHICS DISCLAIMER

All figures, graphics, tables, equations, etc. merged into this translation were extracted from the best quality copy available.

Determination of Kinetic Parameters of Molecular Beam Epitaxy

Zhong Jingchang
(Changchun College of Optics & Fine Mechanics)

Abstract

A kinetic growth model for molecular beam epitaxy (MBE) was discussed. Furthermore, high energy electron diffraction (HEED) was used as a surface characterization method to provide evidence for this model.

GaAs was used as an example to study the growth rate of molecular beam epitaxy. The relation between the growth rate and the flux of Ga was verified by quadrupole mass spectroscopy.

The suitable Ga to Al partial pressure ratio for growing materials such as $Ga_{1-x}Al_xAs$ with specific values of x was investigated theoretically as well as experimentally. Furthermore, the relation between dopant concentration and the corresponding effusion cell temperature was given for Si, Sn and Be.

I. Introduction

Molecular bean epitaxy (MBE) is an ultra high vacuum technique to produce a semiconducting compound through the interaction of a hot molecular beam on the surface of a crystal at a specific temperature. Unlike liquid phase epitaxy, MBE is an unequilibrated growth process. This special mechanism allows low growth rate and temperature. Thus, it is capable of producing large area, uniform semiconductor thin films (on the atomic level). Furthermore, the thickness, chemical composition and dopant level can be rigorously controlled. Important MBE parameters are far more superior to those of liquid and gas phase epitaxy techniques[1]. Because of this reason, it is capable of

producing structure unattainable by the latter techniques. Therefore, MBE has made great progress in the fabrication of microwave components, optoelectronic devices, integrated optical devices, and the theoretically significant quantum trap structure and super lattice structure.

The MBE growth mechanism is being studied in depth. In this work, reaction kinetics, surface morphology and MBE growth rate were discussed experimentally and theoretically. Furthermore, the relations of several important kinetic parameters were determined.

II. MBE Growth Model

Advances in surface analysis created favorable conditions for establishing a growth model for MBE. From HEED pictures one can observe the smoothening process on the substract surface during growth. This phenomenon indicates that the growth mechanism is realized by a two-dimensional stepwise transport process. As atoms adsorbed on the surface increase to the brink of forming a step, any point on the surface may become the origin of the step. The repulsive force between the steps creates acceleration for the atoms to move away from these sources. Hence, the step sources migrate on the surface to reduce the density of steps and to smoothen the surface[2].

Adsorbed atoms may become free atoms again. This desorption process is related to the lifetime of adsorption and the concentration of adsorbed atoms according to the following formula[3]:

received on March 21, 1983

$$\Gamma = n\,\tau, \qquad (1)$$ /258

where Γ is the desorption rate, n is the concentration of adsorbed atoms, and τ is the surface lifetime. In reality, when a beam of atoms at an intensity F is suddenly injected on a

surface in MBE the rate of concentration variation of adsorbed atom is

$$\frac{dn}{dt} = -\frac{n}{\tau} + F, \qquad (2)$$

In this case, the initial condition is n(0) = 0. If we assume that $\tau \neq f(n)$, then the differential equation (2) can be integrated. From equation (1), we get

$$\Gamma(t) = F(1 - e^{-t/\tau}). \qquad (3)$$

From the relation between τ and temperature, the excitation energy E_d for desorption can be determined by

$$\tau = \tau_0 \exp(Ed\ RT), \qquad (A)$$

It was experimentally demonstrated in the MBE of GaAs that the surface lifetime of As is very short on a hot clean GaAs surface. However, it is relatively long on a Ga covered GaAs surface. The desorption of As, in this case, only increases with the consumption of Ga. This indicates that it is necessary to allow Ga adsorption on the GaAs surface in order to adsorb As at high temperatures.

In the actual experiment, elemental arsenic was used as the source. It exists in the AS_4 form. Molecular beams of Ga and As react on hot (100) GaAs surface. As_4 molecules were first adsorbed in a mobile but weakly bound state. The number of adsorbed Ga atoms controls the precipitation and reaction of As_4. One of the situations is that it is desorbed to become a free As_4. The other is to be chemisorbed by meeting a Ga lattice. Two neighboring As_4 molecules in the Ga lattice may react in pairs, i.e., the surface chemical reaction, to form a new desorbed As_4 molecule and four dissociated As atoms to initiate the chemisorption reaction:

$$\begin{aligned} 2As_4(g) &\longrightarrow As_i + As_4(D)\uparrow, \\ As_i + 4V_{As} &\rightleftharpoons 4As_{As}, \end{aligned} \qquad (B)$$

where "*" represents the surface. If an adhesion coefficient - the ratio of the number of atoms adhered to the surface to the total number of incident atoms - is used to describe this process, then an approximate rule may be obtained:

When $F_{As_4} \gg 2F_{Ga}$, i.e., $S_{As_4} \ll 0.5$,
then GaAs grows on the surface where As is stable.

When $F_{As_4} \ll 2F_{Ga}$, i.e., $S_{As_4} \approx 0.5$,
then GaAs grows on the surface where Ga is stable.

From the above analysis one knows that the rate of growth of the MBE GaAs thin film is totally determined by the flux F of the molecular Ga beam incident on the substrate surface (in atoms/cm^2.s), i.e., $R = \alpha.F$ where α is the adhesion coefficient. At the typical MBE growth temperature range (450-620°C) and when As is stable, its numerical value is close to 1. This means that almost all the incident Ga atoms are combined into the expitaxial layer.

There is no generalized mechanism for the incorporation of dopants in MBE. Therefore, each dopant must be handled empirically. Generally, doping is realized by adding the appropriate element in an effusion cell to quantitatively control the electroactive impurities into the growing thin film. The optoelectronic property of the thin film must first depend on the impurity flux across the growth boundary, the probability of atomic adsorption and the surface lifetime. Secondarily, it is also related to the actual combining behavior and the electroactivity of the dopant.

Sn is a very suitable donor dopant for GaAs and $Ga_{1-x}Al_xAs$. The dopant level is proportional to the Sn flux. The maximum level is $10^{19}cm^{-3}$ with very little compensation. However, Sn has the tendency to precipitate preferentially on the surface. The Sn concentration on the surface is several orders of magnitude higher than that in the bulk. The distribution of dopant cannot vary abruptly. It was experimentally discovered that the donor level increased with increasing As_4 flux and decreased with

rising temperature[6]. These results might be interpreted by the fact that the combining rate for Sn is related to the Ga vacancy concentration, which varies with the As_4 flux and the growth /259
temperature. Sn incorporation is also limited by the surface recombination rate. Before a steady state donor concentration is reached in the GaAs thin film, we must build up a steady state number of surface Sn atoms. This number may be 0.1 monolayer.

Si is an amphoteric dopant. In GaAs grown by MBE, Si is a donor in most cases. It is not difficult to reach a flux of 10^{11} atom/cm^2.s to obtain a doping level of $1 \times 10^{16} \sim 5 \times 10^{18}$ cm^{-3}.

Be is an ideal acceptor. In the incorporation, there are no complications such as preferential precipitation and abnormal diffusion. In MBE, the free acceptor level is proportional to the temperature of the Be effusion cell. Therefore, it is a very promising shallow acceptor in the GaAs and $Ga_{1-x}Al_xAs$ systems.

III. Experimental Results and Discussion

A Perkin-Elmer model Φ 400 MBE apparatus was used. The background pressure of the growth chamber was less than 10^{-10} torr. An ionization tube was installed near the substrate to accurately indicate the pressure and the flux.

1. The Growth Rate

According to the model, when the temperature remains unchanged and the adhesion coefficient for Ga is 1 in growing GaAs, the rate of growth R and the Ga flux F have the following relationship:

$$F = R \cdot D \cdot N_0 / M = K \cdot R, \; R = T / t_g,$$

Table 1 Growth Rates Calculated Gallium Fluxes, and Experimentally Obtained Currents of Gallium Ionization

1. 衬底编号	2. 生长温度 (°C)	3. 镓分子束分压 (Torr)	4. 砷分子束分压 (Torr)	5. 生长厚度 (μ)	6. 生长时间 (min)	7. 生长速率 (μm/h)	8. 掺杂浓度 cm⁻³	9. 室温迁移率 (cm²·V⁻¹·s⁻¹)	10. 计算出的镓通量 (原子 cm⁻²·s⁻¹)	11. 四极质谱仪测得的镓电流 (A)
UV-69	484	5.0×10^{-7}	3.3×10^{-6}	1.80	[illegible]	0.9[illegible]	2.5×10^{18} S	5142	6.02×10^{14}	4.01×10^{-7}
Un-71	484	5.5×10^{-7}	3.5×10^{-6}	2.1[illegible]	12[illegible]	1.0[illegible]	7.8×10^{18} Si	4447	6.45×10^{14}	4.35×10^{-7}
UV-8[illegible]	485	5.0×10^{-7}	3.0×10^{-6}	1.95	120	0.98	2.6×10^{18} Si	3425	6.02×10^{14}	4.03×10^{-7}
SW-[illegible]	484	5.0×10^{-7}	3.3×10^{-6}	1.85	120	0.93	—	—	5.71×10^{14}	3.84×10^{-7}
PP-2[illegible]	485	5.1×10^{-7}	3.4×10^{-6}	2.06	120	1.00	1.7×10^{18} Si	2144	6.14×10^{14}	4.10×10^{-7}
QQ-[illegible]	486	5.1×10^{-7}	3.4×10^{-6}	2.20	120	1.10	—	—	6.75×10^{14}	4.52×10^{-7}
CC-44	488	5.5×10^{-7}	3.5×10^{-6}	2.10	118	1.07	1.8×10^{18} Si	4750	6.57×10^{14}	4.39×10^{-7}
CC-45	489	5.1×10^{-7}	3.4×10^{-6}	1.95	120	0.98	3.7×10^{18} Si	3192	6.02×10^{14}	4.02×10^{-7}
CS-[illegible]	487	5.0×10^{-7}	3.3×10^{-6}	2.05	124	0.90	1.3×10^{18} Si	202	$6.[illegible]\times10^{14}$	4.06×10^{-7}
AW-1[illegible]	490	5.1×10^{-7}	3.2×10^{-6}	2.20	1[illegible]	1.[illegible]	2.9×10^{18} Si	124	6.26×10^{14}	4.21×10^{-7}
YY-14	489	$5.[illegible]\times10^{-7}$	3.0×10^{-6}	2.15	[illegible]	[illegible]	1.1×10^{18} B	59	$6.[illegible]\times10^{14}$	$4.1[illegible]\times10^{-7}$

1. substrate number
2. growth temperature (°C)
3. partial pressure of gallium molecular beam
4. partial pressure of arsenic molecular beam
5. growth thickness
6. growth time
7. growth rate
8. dopant concentration
9. room temperature mobility
10. calculated gallium flux
11. gallium current measured by quadrupole mass spectrometer

where D is the density of GaAs, N_0 is the Avogadro's number, M is the molecular weight of GaAs, T is the thickness of GaAs grown, and t_o is the growth time. Hence, the growth rate is linear with respect to the gallium flux. Table 1 shows the growth rates measured at 487 $\pm$ 3°C, the calculated gallium flux values and the /260 ionization currents of the gallium molecular beams as measured by the Faraday cylinder in the quadrupole mass spectrometer. The latter two should only differ by a factor determined by the instrument. From Figure 1 one can see that the Ga ionization current is also linear with respect to the growth rate. The difference between this linear realtionship from that with the calculated Ga flux is in slope.

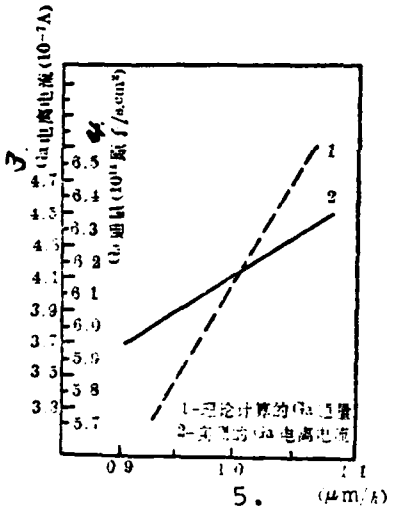

Figure 1. Dependence of the Growth Rate on the Calculated Gallium Flux and on the Experimentally Obtained Gallium Ionization Current

1. calculated theoretical Ga flux
2. measured Ga ionization current
3. Ga ionization current (10^{-7} A)
4. Ga flux (10^{14} atom/s.cm^2)
5. growth ratio (μm/h)

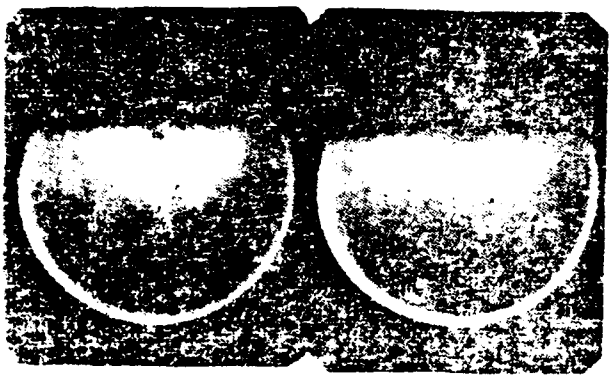

Figure 2. HEED Photographs Before (left) and (right) After Growth

2. Surface Morphology

Figure 2 shows two HEED patterns of the GaAs (100) surface in the MBE growth of GaAs. The substrate surface was finely polished. However, on the atomic scale, the surface is still rough. There are few diffraction fringes and they are coarse. After 2 minutes, the surface became smooth on the atomic scale. Very fine and clear diffraction patterns began to emerge. This is a supporting evidence for the step growth and surface atom migration model.

3. Ratio of Ga to Al Partial Pressure in Growing $Ga_{1-x}Al_x$ As.

When growing $Ga_{1-x}Al_xAs$ with a specific x value, the ratio of Ga to Al partial pressure can be considered as follows:

$$\frac{P(Ga)}{P(Al)} = \frac{1-X}{X} \cdot \frac{S(Ga)}{S(Al)} \cdot \frac{M(Ga)}{M(Al)} \cdot \frac{T(Ga)}{T(Al)}, \qquad (4)$$

where P(Ga) and P(Al) are the partial pressures of Ga and Al, respectively. S(Ga) and S(Al) are the sensitivities of the

onization gauge to Ga and Al, respectively. M(Ga) and M(Al) are he atomic weights of Ga and Al, respectively. T(Ga) and T(Al) re the absolute temperatures of the Ga and Al effusion cells, espectively. Table 2 shows the x values measured by electron nergy dispersion (EDS) spectroscopy at different P(Ga)/P(Al) artial pressure ratios. If the x values in Table 2 are plugged nto equation (4), by taking S(Ga) = 1.7[8], S(Al) = 0.9[8] and (Ga)/T(Al) = 1 to represent the temperature of effusion cells or Ga and Al in the MBE process, a P(Ga)/P(Al) value can be btained corresponding to each measured x value. Table 3 shows he calculated P(Ga)/P(Al) values from equation (4) and the elative deviations between the calculated value and the actual alue used. One can see that the values given by equation (4) re essentially in good agreement with those actually used. The ean relative deviation is 3.2%.

able 2 X Values Measured by the Electron Energy Dispersion Spectroscopy in the Case of Different Ratios of P(Ga)/P(Al) /261

1. 编号	2. 衬底温度 (℃)	3. Ga 分压强 (Torr)	4. Al 分压强 (Torr)	P(Ga)/P(Al)	5. EDS 测量 x 值
ZH-12-5	495	3.2×10⁻⁷	5.1×10⁻⁸	6.275	0.5166
ZH-10-1	491	2.8×10⁻⁷	4.6×10⁻⁸	6.087	0.5275
ZH-9-7	490	2.5×10⁻⁷	4.7×10⁻⁸	5.957	0.5295
ZH-9-7	492	3.0×10⁻⁷	4.8×10⁻⁸	6.125	0.5177
ZH-12-4	490	2.6×10⁻⁷	4.5×10⁻⁸	6.444	0.5054

1. no
2. substrate temperature (°C)
3. Ga partial pressure (Torr)
4. Al partial pressure (Torr)
5. x value measured by EDS

Table 3 Relative Errors Between the Calculated P(Ga)/P(Al) and Corresponding Experimental Values

1. EDS 测出的 x 值	2. 实验采用的 P(Ga)/P(Al)	3. 计算得到的 P(Ga)/P(Al)	4. 相对偏差
0.8106	6.475	6.476	0.1%
0.8275	6.067	6.152	1.1%
0.8298	5.957	6.096	2.3%
0.8175	6.122	6.444	5.2
0.8084	6.442	6.725	4.3%

1. x value measured by EDS
2. P(Ga)/P(Al) used in experiment
3. P(Ga)/P(Al) calculated by equation (4)
4. relative deviation

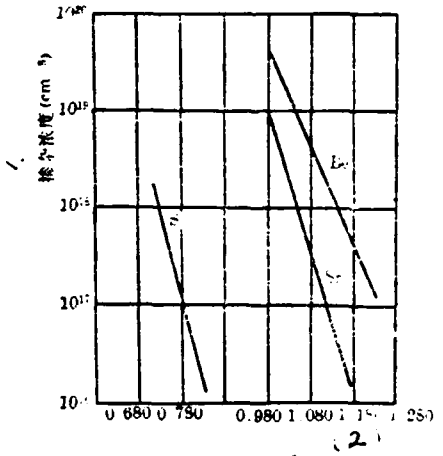

Figure 3 Dependence of Si, Sn, and Be Doping Concentrations on the Temperature of these Dopants

1. dopant level (cm^{-3})
2. reciprocal effusion cell temperature $1000/T(K^{-1})$

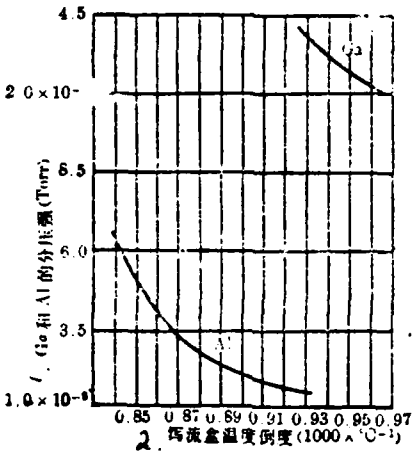

Figure 4. Dependence of the Experimentally Obtained Ga and Al Partial Pressure on the Temperature of Both Elements

1. partial pressures of Ga and Al (Torr)
2. reciprocal effusion cell temperature (1000 x $°C^{-1}$)

4. Relation of Si, Sn and Be Doping Levels and Dopant /262 Temperature

Figure 3 shows the relation between the concentrations of Si, Sn and Be with respect to the effusion cell temperature. One can see that the level could reach n = 2 x $10^{18}cm^{-3}$ for Si, n = 10^{19} cm^{-3} for Sn and P = 5 x $10^{19}cm^{-3}$ for Be.

5. Relation Between Partial Pressures of Ga and Al and Effusion Cell Temperature

Figure 4 shows the relation between partial pressures of Al and Ga with respect to the reciprocal of the effusion cell temperature. This curve is handy in establishing the required partial pressure ratio by controlling the temperature.

IV. Conclusions

In molecular beam epitaxy, the crystal growth process is kinetically limited, instead of quasi-equilibrium limited in liquid phase epitaxy. At a fixed temperature, the growth rate exhibits a linear relationship with respect to the gallium flux. This experimental result is in good agreement with the theory and serves as a good piece of evidence for the growth mechanism. Surface characterization by HEED and quadrupole mass spectrometry also have significant contribution to the establishment of the model. Although only GaAs was investigated, it might be applicable to other III-V semiconductor materials.

Experimentally measured P(Ga)/P(Al) ratios agree with the projected values obtained based on equation (4). From a practical angle, this is a good reference for growing $Ga_{1-x}Al_xAs$ with a specific x value.

This work was conducted under the direction of Dr. M. Gershenzon. Professor of Electrical Engineering and Materials Science, at Southern California University in the U.S. Mr. C. Shannon also assisted in this work. The author wishes to express his gratitude.

References

[1] P.E. Luscher et al.; Electronics, 1980, 53, No.19 (Aug.), 163.

[2] K. Ploog; ((Growth of Crystals)), (Pergamon, 1980), 109-111.

[3] A.Y. Cho, J.R. Arthur; ((Progress in Solid-State Chemistry)), (Pergamon Press, 1975), 157-191.

[4] J.R. Arthur; J. Appl. Phys., 1968, 39, No.8, (Jul),4032.

[5] J.R. Arthur; Surf. Sci., 1974, 43, 449.

[6] K. Ploog et al.; J. Vac. Sci. Technol., 1979, 16, No.2 (Mar-Apr), 290.

[7] M.V. McLevige et al.; Appl. Phys. Lett.; 1978, 33, No.2 (Jul), 127.

[8] G.L. Weissler, R.W. Carson; ((Vacuum Physics and Technology)), (Academic Press, 1979), Vol.14, 74.

END

FILMED

7-85

DTIC